Thickness Dependence of the Effective Masses in a Strained Thin Silicon Film

Viktor Sverdlov[1], Oskar Baumgartner[1], Thomas Windbacher[1], Franz Schanovsky[2], and Siegfried Selberherr[1]
[1]Institute for Microelectronics
[2]Christian Doppler Laboratory for TCAD at the Institute for Microelectronics
TU Wien
Gußhausstraße 27-29/E360
A-1040 Wien, Austria
{sverdlov|baumgartner|windbacher|schanovsky|selberherr}@iue.tuwien.ac.at

***Abstract*— By comparing results obtained with the density-functional method, empirical pseudo-potential method, and empirical tight-binding method it is demonstrated that the conduction band structure is accurately described by the two-band k·p model. The later model is used to investigate the subband structure in ultra-thin (001) silicon films. It is demonstrated for the first time that the unprimed subbands with the same quantum number are not equivalent in ultra-thin films and develop different effective masses along [110] and [-110] directions. Using the two-band k·p model the dependence of the subband effective masses on strain and thickness is calculated. It is shown that the mass along tensile stress in [110] direction decreases with strain guaranteeing current enhancement in thin films. Shear strain also introduces large splitting between the unprimed subbands with the same *n*. Finally, the dependence of the effective masses in primed subbands is calculated and found to agree well with recent pseudopotential calculations.**

Keywords - two-band k·p model, shear strain, subband splitting, strain and thickness dependent effective masses

I. INTRODUCTION

The rapid increase in computational power and speed of integrated circuits is supported by the continuing size reduction of semiconductor devices' feature size [1]. With scaling apparently approaching its fundamental limits, the semiconductor industry is facing critical challenges and new engineering solutions are required to improve CMOS device performance. Strain-induced current enhancement is one of the most attractive solutions to increase the device speed and will maintain its key position among possible technology innovations. In addition, a multi-gate MOSFET architecture is expected to be introduced for the 22nm technology node. Combined with a high-k dielectric/metal gate technology and strain engineering, a multi-gate MOSFET appears to be the ultimate device for high-speed operation with excellent channel control, reduced leakage currents, and low power budget.

Uniaxial [110] strain modifies the transversal effective masses of the two (001) valleys [2]. The mass change is accurately described by the two-band **k·p** model of the conduction band [3]. The two-band **k·p** model [2-4] provides a general framework to compute the subband structure, in particular the dependence of the subband effective masses on shear strain. In case of a square potential well with infinite walls, which is a good approximation for the confining potential in ultra-thin Si films, the dispersion equations were obtained [5], however, an accurate analysis of the electron subband structure is still missing.

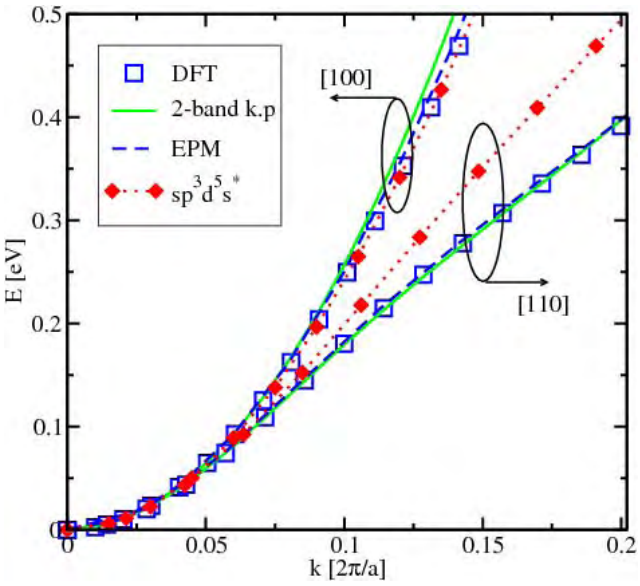

Figure 1. Comparison of the conduction band of silicon computed with DFT, EPM, $sp^3d^5s^*$, and the k·p method. The k·p model is accurate up to an energy of 0.5eV.

Here we describe the subband structure and the dependence of the subband effective masses on strain and thickness t by solving the two-band **k·p** model in a thin (001) film under [110] tensile strain numerically. This allows an analysis of subband energies and effective masses for both primed and unprimed subbands in (001) silicon films.

II. THE TWO-BAND K·P MODEL

The two-band **k·p** model was suggested first in [2] to explain experimentally observed strain dependence of the cyclotron effective mass on the orientation of the external magnetic field. It can be written as

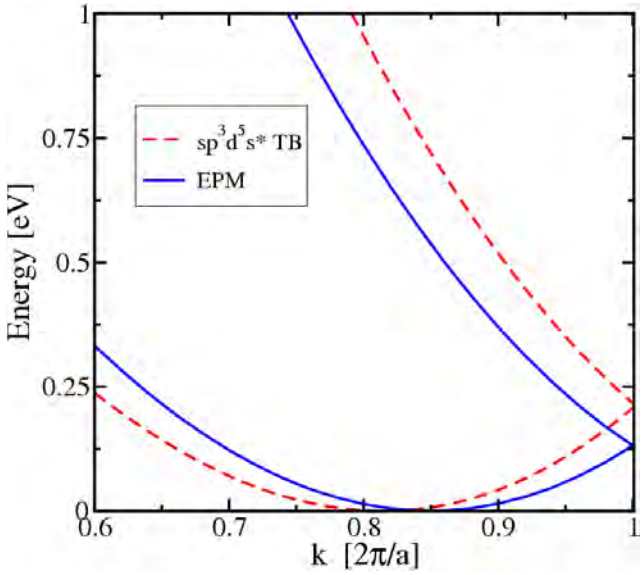

Figure 2. Conduction band dispersion along the $\Gamma - X$ direction obtained with the EPM and the TB methods. Because of the minimum position found further away from the *X*-point, the gap between the two conduction bands at the minimum obtained with the TB method [8] is two times larger.

$$H = \left(\frac{\hbar^2 k_z^2}{2m_l} + \frac{\hbar^2 (k_x^2 + k_y^2)}{2m_t} \right) I + \left(D\varepsilon_{xy} - \frac{\hbar^2 k_x k_y}{M} \right) \sigma_z + \frac{h^2 k_z k_0}{m_l} \sigma_y \quad (1)$$

where $\sigma_{y,z}$ are the Pauli matrices, *I* is the 2x2 unity matrix, m_t and m_l are the transversal and the longitudinal effective masses, $k_0 = 0.15 \times 2\pi / a$ is the position of the valley minimum relative to the *X* point in unstrained Si, ε_{xy} denotes the shear strain component, $M^{-1} = m_t^{-1} - m_0^{-1}$, and *D*=14 eV is the shear strain deformation potential [2-4]. It was demonstrated in [3] that the form of the Hamiltonian suggested is the only one compatible with the symmetry of the Brillouin zone in the vicinity of the *X*-point. The two-band Hamiltonian results in the following dispersions:

$$E = \frac{\hbar^2 k_z^2}{2m_l} + \frac{\hbar^2 (k_x^2 + k_y^2)}{2m_t} \pm \sqrt{\left(\frac{\hbar^2 k_z k_0}{m_l} \right)^2 + \delta^2} \quad (2)$$

where the negative sign corresponds to the lowest conduction band, and $\delta^2 = (D\varepsilon_{xy} - \hbar^2 k_x k_y / M)^2$. In (1) and (2) energies and k_z are counted from the corresponding values at the *X*-point.

A comparison between the results of band structure calculations of silicon obtained with different methods is shown in Fig.1. The empirical pseudo-potential method (EPM) [4,6] gives the most accurate results as compared to the density functional based calculations (DFT) performed with VASP [7]. The empirical tight-binding sp3d5s* model with parameters from [8] seems to underestimate the anisotropy of the conduction band. The reason for such a behavior is displayed in Fig.2. The minimum of the conduction band within the tight-binding model is located further away from the *X*-point than k_0. This leads to the gap between the two bands at the minimum of the lowest conduction band which is nearly two times larger than the corresponding gap from EPM calculations. Since the warping of the conduction band is determined by the band interaction, the larger gap results in less coupling and lower degree of anisotropy.

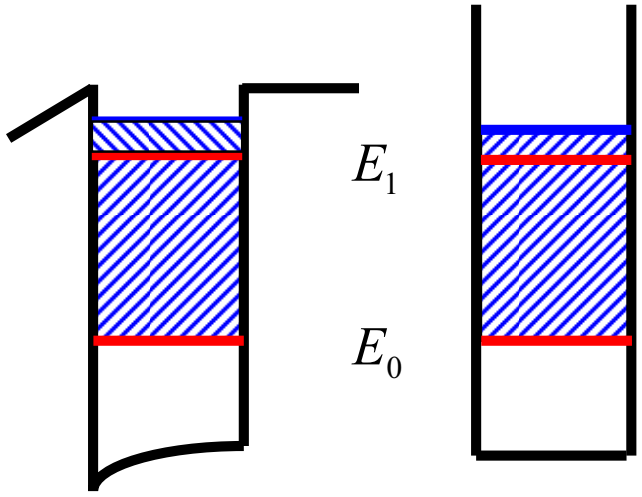

Figure 3. Scetch of the potential profile in a thin body of a single-gate MOSFET (left) and its approximation by the square well potential with infinite potential walls (right).

As demonstrated in Fig.1, the two-band **k·p** model adequately describes the conduction band dispersion up to anenergy of 0.5eV and can therefore be used to analyze the subband structure in thin silicon films.

III. Unprimed Subbands in (001) Thin Films

In order to analyze the subband structure in (001) oriented thin silicon films we first approximate the film potential by the square well potential with infinite potential walls as illustrated in Fig.3. Although not exact, this is a good approximation for thin films. The Hamiltonian for unprimed subbands inside the film is in the form (1), with $k_z = -i\frac{d}{dz}$. The wave function is a spinor, with both components equal to zero at the film interfaces. The dispersion relations for unprimed subbands are obtained by substituting $k_z = k_0(x_n + y_n)$ into (2), where x_n and y_n are found from the following equations [5]:

$$\sin(y_n k_0 t) = \pm \frac{\eta y_n \sin(x_n k_0 t)}{\sqrt{(1 - y_n^2)(1 - \eta^2 - y_n^2)}}, \quad (3a)$$

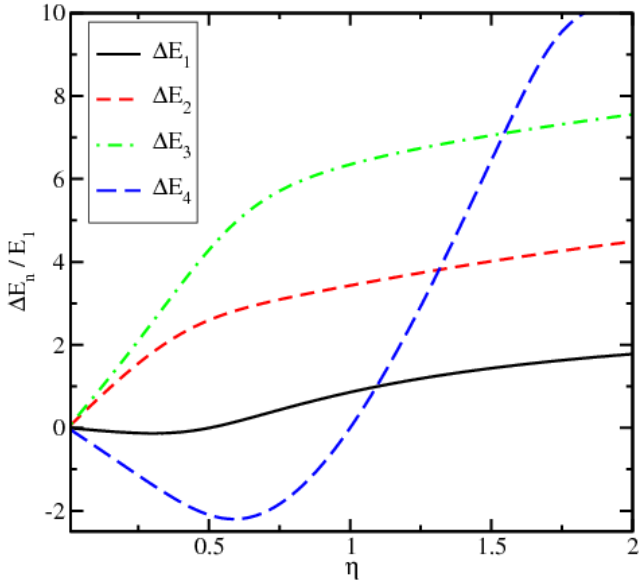

Figure 4. Strain-dependent splitting between the minima of the unprimed subbands with the same n in a film with the thickness t=4.3nm normalized to the subband energy of the ground subband in relaxed film. Depending on the parameters, the splitting dependence on strain may be nonmonotonic.

$$x_n = \sqrt{\frac{1-\eta^2-y_n^2}{1-y_n^2}}\,. \qquad (3b)$$

Without stress when $\eta = m_l\delta/(\hbar k_0)^2 = 0$ the k_z dispersion (2) is parabolic, and the standard quantization conditions $y_n = \pi n/(k_0 t)$ are obtained. For arbitrary η (3) must be solved numerically.

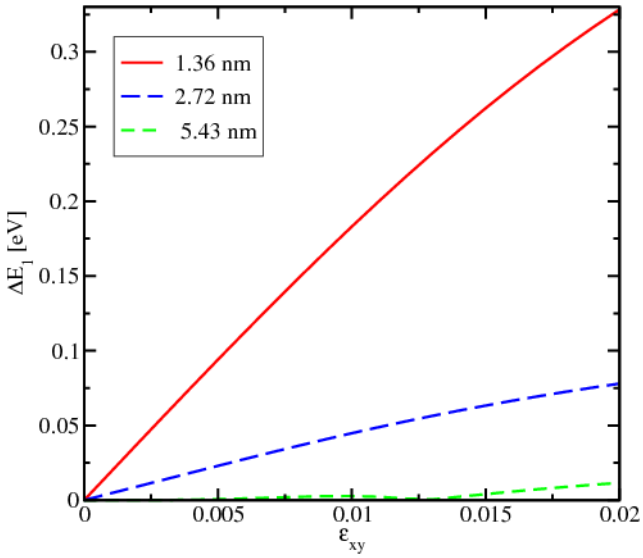

Figure 5. Shear strain induced splitting of the ground subbands, for several film thicknesses. In ultra-thin films the splitting is larger than kT for moderate stress.

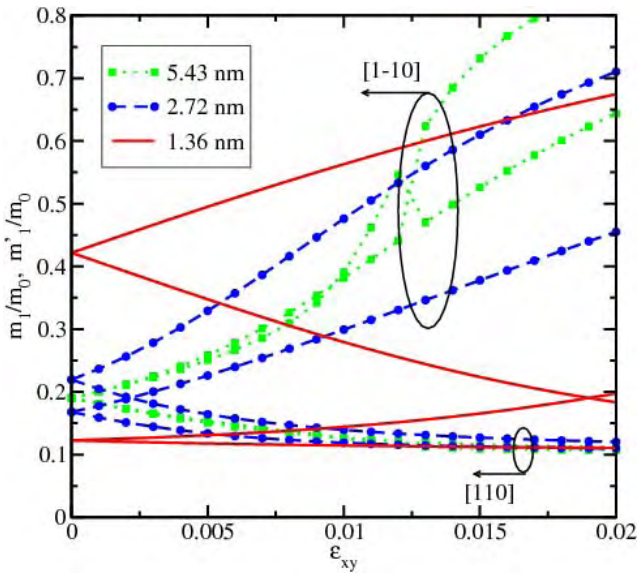

Figure 6. Effective masses of the two ground subbands. In ultra-thin films the effective masses of the two ground subbands are different even without stress.

IV. Results

The splitting between the unprimed subbands with the same number n normalized to the ground subband energy in unstrained films for a film of the thickness t=4.3nm is shown in Fig.4 as function of shear strain. The dependence is not monotonic and strongly depends on the subband number. Even for the ground subbands with n=1 the splitting is comparable to the subband energy at large strain values. The subband splitting increases rapidly with the film thickness decreased as demonstrated in Fig.5. For ultra-thin body films the splitting can reach a value comparable to $k_B T$ already at moderate strain values.

The dependence of the subband effective masses in [110] and [1-10] directions on tensile strain along [110] direction is shown in Fig.6. Like in the bulk [4], the effective mass decreases in the tensile strain [110] direction guaranteeing enhancement of current and mobility by shear strain in thin films. However, the effective masses of the two unprimed subbands with the same number become nonequal in ultra-thin films even without strain. Fig.7 demonstrates a strong dependence of the effective masses of the two ground subbands on the film thickness t. Subbands are, however, non-parabolic as shown in the inset to Fig.7 where the equipotentials of the corresponding dispersion relations for a t=1.36nm thin film are shown.

In order to understand these results, we solve (3) by perturbation including terms linear in η :

$$E_n^{\pm} = \frac{\hbar^2}{2m_l}\left(\frac{\pi n}{t}\right)^2 + \hbar^2\frac{k_x^2+k_y^2}{2m_t} \pm \left(\frac{\pi n}{k_0 t}\right)^2 \frac{\left|D\varepsilon_{xy} - \frac{\hbar^2 k_x k_y}{M}\right|}{k_0 t\left|1-(\pi n/k_0 t)^2\right|}\sin(k_o t) \qquad (4)$$

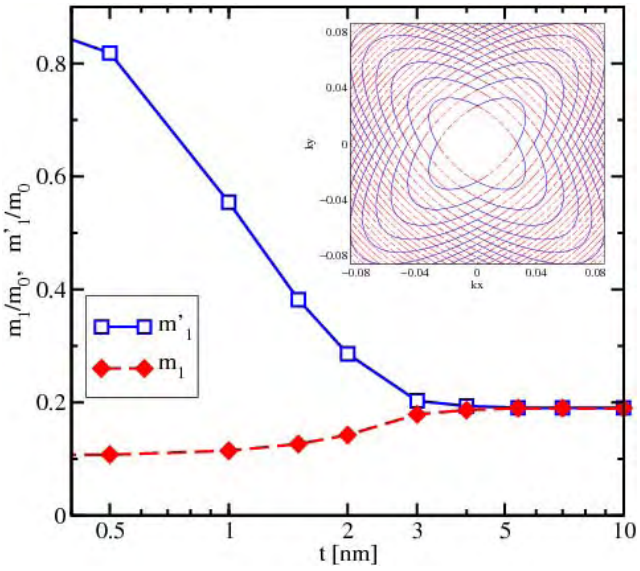

Figure 7. Effective masses of the two ground subbands as a function of film thickness. Inset: Contour plots of their dispersions.

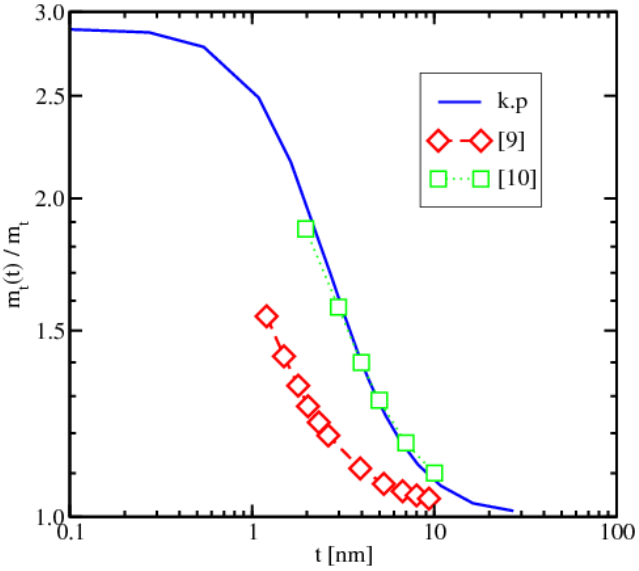

Figure 8. The thickness dependence of the effective mass of the lowest primed subbands computed with the two-band k·p model (solid line) is in excellent agreement with the full-band calculations [5].

It follows from (4) that the splitting between the subbands is linear in shear strain and is inversely proportional to the film thickness in the third power. Expression (4) also describes the effective mass dependence on film thickness along [110] and [1-10] directions:

$$m_{(1,2)} = \left(\frac{1}{m_t} \pm \frac{1}{M} \left(\frac{\pi n}{k_0 t} \right)^2 \frac{\sin(k_o t)}{k_0 t \left| 1 - (\pi n / k_0 t)^2 \right|} \right)^{-1} \qquad (5)$$

Finally, by analogy, considering confinement along the *x* axes, (1) allows to calculate the dependence of the effective masses on thickness in primed subbands. The effective mass dependence follows the trend predicted in [9]. Excellent agreement with the recent pseudo-potential based calculations [10] is demonstrated in Fig.8.

CONCLUSION

It is shown that the two-band **k·p** model accurately describes the conduction band in silicon and can be used to investigate the subband structure in thin silicon films. It is demonstrated that the unprimed subbands with the same quantum number become nonequivalent in thin silicon (001) films by developing different dispersions along [110] and [-110] directions characterized by different effective masses. When shear strain is applied, the energy splitting between the two subbands with the same *n* appears, which becomes comparable to the temperature in ultra-thin films already for moderate stress. Strain dependence of the effective masses is calculated. For primed subbands the calculated dependence of the effective mass on thickness is shown to be in excellent agreement with results of pseudo-potential calculations.

ACKNOWLEDGEMENTS

This work was supported in part by the Austrian Science Fund FWF, projects P19997-N14 and I79-N16.

REFERENCES

[1] S.Natarjan, M.Armstrong, H.Bost, *et al.*, "A 32nm logic technology featuring 2nd-generation high-k + metal-gate transistors, enhanced channel strain and 0.171μm^2 SRAM cell size in a 291Mb array", *IEDM* 2008, pp.941-943.

[2] J.C. Hensel, H. Hasegawa, and M. Nakayama, "Cyclotron Resonance in Uniaxially Stressed Silicon. II. Nature of the Covalent Bond", *Phys.Rev.* **138**, A225-A238 (1965).

[3] G.L. Bir and G.E. Pikus, Symmetry and Strain-Induced Effects in Semiconductors, J.Wiley & Sons, NY, 1974.

[4] E. Ungersboeck, S. Dhar, G. Karlowatz, *et al.*, "The Effect of General Strain on the Band Structure and Electron Mobility of Silicon", *IEEE Transactions on Electron Devices* **54**, pp. 2183-2190 (2007).

[5] V. Sverdlov and S. Selberherr, "Electron Subband Structure and Controlled Valley Splitting in Silicon Thin-Body SOI FETs: Two-Band k.p Theory and Beyond", *Solid State Electronics* **52**, 1843-1851 (2008).

[6] M. Rieger and P. Vogl, "Electronic-Band Parameters in Strained $Si_{1-x}Ge_x$ Alloys on $Si_{1-y}Ge_y$ Substrates", *Phys.Rev.* B **48**, 14275-14287 (1993).

[7] Vienna Ab-initio Simulation Program: G.Kresse, J. Hafner, *Phys.Rev*. B **47**, 558 (1993); ibid. B **49**, 14251 (1994); G.Kresse and J. Furthmueller, *Phys.Rev*. B **54**, 11169 (1996); *Computs.Mat.Sci.* **6**, 15 (1996).

[8] T.B. Boykin, G. Klimeck, F. Oyafuso, "Valence band effective-mass expressions in the $sp^3d^5s^*$ empirical tight-binding model applied to a Si and Ge parametrization", *Phys.Rev.* B **69**, 115201 (2004)

[9] A. Martinez, K. Kalna, P. V. Sushko, *et al.*,"Impact of Body-Thickness-Dependent Bandstructure on Scaling of Double Gate MOSFETs: a DFT/NEGF study", *IEEE Trans. Nanotechnol.* **8**, No. 2, pp. 159-166. (2009).

[10] L.-L.P.J van der Steen, D. Esseni, P. Palestri, *et al.*, "Validity of the Parabolic Effective Mass Approximation in Silicon and Germanium n-MOSFETs With Different Crystal Orientations", *IEEE Transactions on Electron Devices* **54**, pp. 1843-1851 (2007).